



Optimized waste tea activated carbon for adsorption of Methylene Blue and Acid Blue 29 dyes using response surface methodology

M. Auta, B.H. Hameed*

School of Chemical Engineering, Engineering Campus, Universiti Sains Malaysia, 14300 Nibong Tebal, Penang, Malaysia

ARTICLE INFO

Article history:

Received 11 July 2011

Received in revised form

20 September 2011

Accepted 21 September 2011

Keywords:

Optimization

Isotherm

Kinetics

Adsorption

Thermodynamics

Activation

ABSTRACT

Waste tea activated carbon (WTAC) was produced at optimum conditions for adsorption of both anionic and cationic dyes. The WTAC was produced through chemical activation with potassium acetate for adsorption of Methylene Blue (MB) and Acid Blue 29 (AB29) dyes. Response surface methodology statistical technique was used to optimize the preparation conditions which were activation temperature, activation time and chemical impregnation ratio (IR); with percentage yield and removal as the targeted responses. The optimal conditions obtained for good percentage yield and removal of the two dyes were at 800 °C, IR 1.4 and 120 min. The high surface area of 854.30 m²/g and mesoporous adsorbent prepared gave good adsorption capacities of 453.12 and 554.30 mg/g for AB29 and MB, respectively. Adsorption data were modeled using Langmuir, Freundlich and Temkin adsorption isotherms; the adsorption of MB and AB29 on WTAC both obeyed Langmuir model and, pseudo-second-order kinetics was the order that best described the two adsorption processes. The WTAC produced can be used effectively to salvage pollution problems posed by both anionic and cationic dyes in the environment.

© 2011 Elsevier B.V. All rights reserved.

1. Introduction

Conscientious effort has been made by researchers to develop a cheaper, more effective and environmental friendly activated carbon that are comparable with commercially available ones. This has taken various dimensions which includes using various precursors such as agricultural waste based materials, clays, polyethenes and so on; devising various methods of preparations; and, use of various chemicals for activation. Activated carbons have been useful in adsorption processes for decades with outstanding excellent records [1]. Adsorption processes have been used in various fields which include medicine, environment, oil and gas and so on for removal of metals, dyes, pesticides, storage, and oil spillage control [2].

Chemical activation, a method other than physical activation which is one of the two main processes for the preparation of activated carbon has found immense applications. This is because the method is energy and time saving and, yields good results of product. The process requires impregnation of precursor or charred carbon with activating agent and pyrolysed; this help in developing the surface area as well as the pores. Various activating agents like H₂SO₄, HCl, H₃PO₄, KOH, NaOH, ZnCl₂, and K₂CO₃ have been

used [3,4]. The choice and manner of usage depends on nature of precursor and the performance of the activating agent [5].

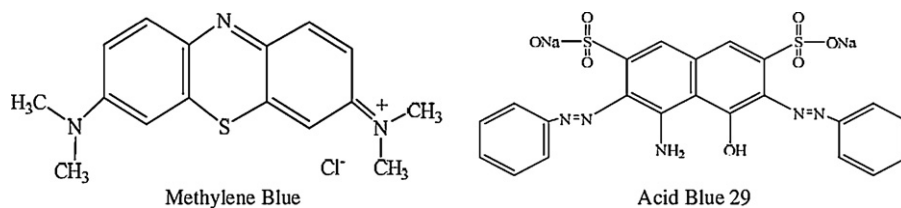
Potassium hydroxide is one of the best activating agents that enhances development of good surface area and pore of precursors in the cause of production of activated carbon. The reaction of potassium hydroxide and carbon has numerous stages of developing pores of chars. Its contribution during activation brought about the discovery of CH₃CO₂K which is also a good activating agent [4].

One of the major aims of engineering researches apart from efficiency and efficacy of output is economic viability. Experimental design technique enables researchers to rationalize experiments thereby cutting cost and creating more interest in research field by alleviating the rigors often experienced by researchers. This statistical tool assists in bringing to lime light factors optimized. Good activated carbon production is based upon a number of conditions which must be consciously and adequately considered. Response surface methodology has been useful in getting optimal result for interaction amongst factors as reported by many researchers [6–9].

In our earlier studies [4], we reported the possibility of using potassium acetate as an activating agent for preparation of activated carbons but did not optimize the production process. On this premise, this study was carried out to optimize the conditions paramount for the production of activated carbon from waste tea for large scale application. Central composite design (CDD) under response surface methodology (RSM) was chosen to evaluate the interaction of operating conditions such as activating agent to precursor ratio, activation temperature and activation time; and the

* Corresponding author. Tel.: +60 45996422; fax: +60 45941013.

E-mail address: chbassim@eng.usm.my (B.H. Hameed).



Scheme 1. Molecular structures of MB and AB29.

optimized waste tea activated carbon (WTAC) prepared was of good yield and also gave high percentage removal of Methylene Blue (MB) and Acid Blue 29 dye (AB29).

2. Materials and methods

2.1. Raw material

Potassium acetate, Methylene Blue (MB) and Acid Blue (AB29) dyes were purchased from Merck Chemicals Company Malaysia, Sigma-Aldrich chemicals Malaysia and Aldrich Company Inc. USA, respectively; the chemicals were used without further purification. The chemical formula and molecular weights for MB and AB29 are $C_{16}H_{18}N_3S$, 319.85 g/mol and $C_{22}H_{14}N_6Na_2O_9S_2$, 616.49 g/mol, respectively; and the molecular structure of MB and AB29 are shown in Scheme 1. Waste tea was obtained from Engineering campus cafeteria, Universiti Sains Malaysia, which was purified by washing with hot distilled water several times and then dried until there was no weight difference.

2.2. Preparation of activated carbon

Waste tea activated carbon was prepared with potassium acetate as activating agent under the consideration of the following factors: impregnation ratio, of activating agent to waste tea (0.3–2.5), temperature of activation (500–800 °C) and time of activation (60–150 min). Typically, the dried purified waste tea of particle sizes between 200 and 500 μm was measured and mixed with the activating agent, activated at temperature and time as was determined by the design of experiment (DOE) table. The detailed preparation method is contained in our previous work [4]. The prepared adsorbent was washed with distilled water until a neutral pH was attained and then stored in airtight container for further

use. The precursor was mixed with the activating agent using the following relationship:

$$IR = \frac{\text{dried weight of } CH_3COOK}{\text{dried weight of precursor}}$$

The preparation of the adsorbent was with strict adherence to the DOE table as shown in Table 1.

2.3. Design of experiments using response surface methodology

Central composite design (CCD) amongst other designs under RSM was used to study the individual and synergetic effect of the three factors towards the responses. It is a method that helps to prune unnecessary experiments and checkmate whether or not there is synergy amongst the factors. CCD is characterized by three operations namely: $2n$ axial runs, 2^n factorial runs and six center runs. For this case, it translated to 6 axial points, 8 factorial points and 6 replicates at the center which gives a total of 20 experiments.

$$\text{Total number of experiments} = 2^n + 2n + n_c$$

where n is the number of factors, n_c is the number of center points (six replicates).

The usual code of ± 1 was used to represent the eight factorial points, the six axial points located at $(\pm\alpha, 0, 0)$, $(0, \pm\alpha, 0)$, $(0, 0, \pm\alpha)$, and the six replicates located at the center $(0, 0, 0)$ were run. Alpha (α) is the distance of the axial point from center had its value fixed at $\alpha = 1.682$. The coded points and their corresponding values are presented in Table 2. This value of rotatability α , which depends on the number of points in the design of the factorial portion, was obtained from the following equation [9]:

$$\alpha = N_p^{1/4} \quad (1)$$

Table 1
Experimental design matrix using RSM for preparation of WTAC.

Run	Activated carbon preparation variable			Activated carbon yield, Y_2 (%)	AB29 removal, Y_{AB29} (%)	MB removal, Y_{MB} (%)
	IR, x_1	Activation temperature, x_2 (°C)	Activation time, x_3 (min)			
1	0.75	561	78	27.35	34.19	34.19
2	2.05	561	78	36.40	38.03	38.03
3	0.75	739	78	23.45	50.47	49.47
4	2.05	739	78	33.20	67.75	99.47
5	0.75	561	132	27.70	30.56	21.73
6	2.05	561	132	39.10	35.69	35.70
7	0.75	739	132	30.75	90.82	98.50
8	2.05	739	132	27.35	97.15	99.12
9	0.3	650	105	28.00	30.44	27.52
10	2.5	650	105	35.30	31.25	41.25
11	1.4	500	105	32.45	19.34	34.45
12	1.4	800	105	31.20	99.66	99.72
13	1.4	650	60	31.35	30.32	33.35
14	1.4	650	150	34.65	40.87	46.91
15	1.4	650	105	37.20	52.21	35.85
16	1.4	650	105	37.20	55.45	35.88
17	1.4	650	105	37.20	48.98	36.82
18	1.4	650	105	37.20	55.66	35.89
19	1.4	650	105	37.20	48.23	36.02
20	1.4	650	105	37.20	55.72	34.99

Table 2
Independent variables and their coded levels for the central composite design.

Variables (factors)	Code	Unit	Coded variable levels				
			$-\alpha$	-1	0	$+1$	$+\alpha$
Impregnation ratio (IR)	x_1	–	0.3	0.75	1.4	2.05	2.5
Activation temperature	x_2	°C	500	561	650	739	800
Activation time	x_3	min	60	78.24	105	132	150

where $N_p = 2^k$ is the number of points in the cube portion of the design, k is the number of factors.

The optimal conditions for the responses yield and percentage removal of both MB and AB29 were determined using the optimal model predictor quadratic equation given as:

$$Y = b_0 + \sum_{i=1}^n b_{ii}x_i + \left(\sum_{i=1}^n b_{ii}x_i \right)^2 + \sum_{i=1}^{n-1} \sum_{j=i+1}^n b_{ij}x_i x_j \quad (2)$$

where Y is the predicted response, b_0 is the constant coefficients, b_{ii} is the quadratic coefficients, b_{ij} is the interaction coefficients and x_i, x_j are the coded values of the variables considered. The regression analysis to fit the equations for both responses developed and for the evaluation of the statistical significance of the equation obtained with the aid of the experimental data were analyzed using Design Expert software (statistical) version 6.0.6 (STAT-EASE Inc., Minneapolis, USA). The characteristics of the reliability of the analysis carried out was measured by the variability in the observed responses values expressed by coefficient of determination R^2 , the probability P -value (95% confidence level) and Fisher's test.

The two responses, yield of the WTAC and percentage removal of MB and AB29 were determined in the following ways.

The yield of the WTAC produced after the waste tea precursor was subjected to activation, washing and drying; was calculated as:

$$\text{Yield (\%)} = \frac{\text{weight (g) of dried activated carbon produced}}{\text{weight (g) of dried precursor used}} \times 100 \quad (3)$$

In a typical batch experiment, 0.2 g of WTAC (adsorbent) was placed in a set of 250 mL Erlenmeyer flasks containing 200 mL of 200 mg/L initial adsorbate concentration. At the dye solution natural pH, the flasks were placed in an isothermal shaker at 30 °C at shaker speed of 140 rpm until equilibrium was attained. At equilibrium, the concentration of the MB/AB29 remaining in the solution was determined using UV–vis spectrophotometer (Shimadzu UV/Vis 1700, Japan) at maximum wavelength, $\lambda_{\text{max}} = 668$ nm of MB and 602 nm of AB29. The dye removal (%) was calculated as follows:

$$\text{Dye removal (\%)} = \frac{\text{initial dye concentration} - \text{final dye concentration}}{\text{initial dye concentration}} \times 100 \quad (4)$$

2.4. Characterization of the waste tea activated carbon

The analysis carried out were Brunauer–Emmett–Teller (BET) to determine the surface area and porosity of the WTAC, pH point of zero charge (pHzpc), surface morphology of the adsorbent was determined through scanning electron microscopy (SEM), and Fourier transform infrared spectroscopy (FT-IR) technique was used to examine the surface functional groups responsible for dyes adsorption.

The BET was carried out by nitrogen adsorption-desorption method using nitrogen temperature (-196 °C) with an autosorb

BET apparatus, Micrometrics ASAP 2020, surface area and porosity analyzer. The analysis procedure was automated and operated with static volumetric techniques. The samples were first degassed at 200 °C for 2 h before each measurement was recorded.

The pH zero surface charge pHzpc of the WTAC characteristics was carried out by using the solid addition method [10]. Three initial concentrations of KNO_3 (0.1, 0.01, 0.001 mol/dm³) of 40 mL each were measured into eighteen 100 mL conical flasks with glass stoppers and 0.2 g of WTAC added. The pHs of the prepared KNO_3 solutions were adjusted between 2 and 12 with either 0.1 M of KOH or 0.1 M H_2SO_4 . The samples were shaken for 12 h at 135 rpm. At the expiration of time, when equilibrium was established between the KNO_3 solution and the WTAC, the final pH readings were noted. The final pH values were plotted against the initial pH values of the solution and at the point where plateau like feature occurred on the plot, the corresponding pH reading was noted and taken as the pHzpc of WTAC. This is similar to the method used by Al-Degs et al. [11]. The surface morphology of the samples was examined using a scanning electron microscope (JEOL, JSM-6460 LV, Japan) with an Oxford INCA/ENERGY-350 microanalysis system.

The FT-IR analyses were performed on the samples using a Perkin-Elmer spectrum GX Infrared Spectrometer with resolution of 4 cm⁻¹ in the range of 4000–400 cm⁻¹. The sample and analytical grade potassium bromide (KBr) were dried at 100 °C overnight prior to the analysis. The KBr and sample were prepared with the disc technique using a finely ground mixture of 0.25 mg of sample and 100 mg of KBr.

2.5. Adsorption equilibrium and kinetic studies

Adsorption studies were conducted to investigate the effect of contact time, initial dye concentration, effect of temperature and initial dye concentration on adsorption of both MB and AB29 on WTAC.

Adsorption equilibrium studies were performed in a set of Erlenmeyer flasks (250 mL) containing 200 mL of the dye solutions at different initial concentrations (50–350 mg/L). About 0.2 g (1–3 mm) of WTAC adsorbent was added, mixed and placed in water bath isothermal shaker at 30 °C for 12 h, and shaker speed of 140 rpm to attain equilibrium. The water-bath shaker temperature was adjusted to 40 °C and 50 °C, and similar procedure was repeated with another set of flasks containing same different initial dye concentrations (50–350 mg/L). The flasks were afterwards removed from the shaker for determination of final concentration of the solution using UV–vis spectrophotometer (Shimadzu UV/Vis 1601 spectrophotometer, Japan) at maximum wavelength of 668 nm and 602 nm for MB and AB29, respectively. The amount of the dye adsorbed at time t , at equilibrium Q_e (mg/g) was calculated using the following equation:

$$Q_e = \frac{(C_0 - C_e)V}{W} \quad (5)$$

where C_0 and C_e (mg/L) are the liquid-phase concentration of the dye at the initial and equilibrium, respectively; V (L) is the volume of the solution; and W (g) is the weight of the dry adsorbent used.

In order to study the kinetics of the adsorption process, concentration of the dye solution was determined at intervals of time.

The amount of the dye adsorbed at time t , Q_t (mg/g) was calculated using equation:

$$Q_t = \frac{(C_0 - C_t)V}{W} \quad (6)$$

where C_0 and C_t (mg/L) are the liquid-phase concentration of the dye at the initial and any time t , respectively; V (L) is the volume of the solution; and W (g) is the weight of the dry adsorbent.

The effect of initial pH (2–12) on the adsorption of the MB/AB29 dye by WTAC was carried out by adjusting the pH of the solution with 0.1 M HCl and 0.1 M NaOH solutions. The study was conducted in a set of 250 mL Erlenmeyer flasks charged with 200 mg/L and 0.20 g of the dye concentration and WTAC, respectively at a temperature of 30 °C for 12 h.

3. Results and discussion

3.1. Design of experiments using response surface methodology

The development of a polynomial regression equation for analysis of correlation between WTAC yield and its ability to remove both MB and AB29 was done using CCD. Final coded factors empirical models with exclusion of insignificant terms for the yield Y_1 and MB/AB29 adsorption on WTAC Y_{MB}/Y_{AB29} are given as equations Y_1 , Y_{MB} and Y_{AB29} , respectively. The relative predictive power of the quality of the models R^2 were found within the range of desirability as 0.945 (yield), 0.914 (MB) and 0.92 (AB29). The relatively high nature of these values was an indication of qualitative agreement between the predicted values and the experimental values obtained for the three variables under study.

$$Y_{MB} = 35.44 + 6.61x_1 + 23.92x_2 + 4.15x_3 + 1.95x_1^2 + 13.51x_2^2 + 3.98x_3^2 + 3.95x_1x_2 - 5.06x_1x_3 + 7.94x_2x_3 \quad (7)$$

$$Y_{AB29} = 52.47 + 2.49x_1 + 22.18x_2 + 6.32x_3 - 5.11x_1^2 + 5.03x_2^2 - 1.86x_3^2 + 1.83x_1x_2 - 1.21x_1x_3 + 9.46x_2x_3 \quad (8)$$

$$Y_1 = 37.24 + 2.86x_1 - 1.31x_2 + 0.74x_3 - 2.21x_1^2 - 2.15x_2^2 - 1.74x_3^2 + 1.76x_1x_2 - 1.35x_1x_3 - 0.20x_2x_3 \quad (9)$$

The percentage yield was in the range of 23.45–39.10% while the percentage removal for MB and AB29 by the WTAC were in the ranges of 21.73–99.72% and 19.34–99.66%, respectively; these can be found on the total experimental design matrix and the values of the responses obtained presented in Table 1. Quadratic model was used as selected by the software for the two responses. The models were selected based on the highest order polynomials where the additional terms were significant and the models were not aliased, according to the sequential model sum of squares. The six replicate variables at the center points, run 15–20 were conducted to determine the experimental error and the reproducibility of the data.

3.2. Analysis of variance (ANOVA)

The ANOVA was used to further emphasize the adequacy of the models and their significance. The mean squares in the ANOVA for the surface response quadratic models were obtained by dividing the sum of the squares of each of variation sources, the model and the error variance by the respective degrees of freedom. The fishers variance ratio F -value and $\text{Prob} > F$ for the yield of WTAC were 7.64 and 0.0019, respectively. The model for yield revealed that x_1 , x_1^2 , x_2^2 , x_3^2 and x_1x_2 were significant whereas x_2 , x_3 , x_1x_3 , and

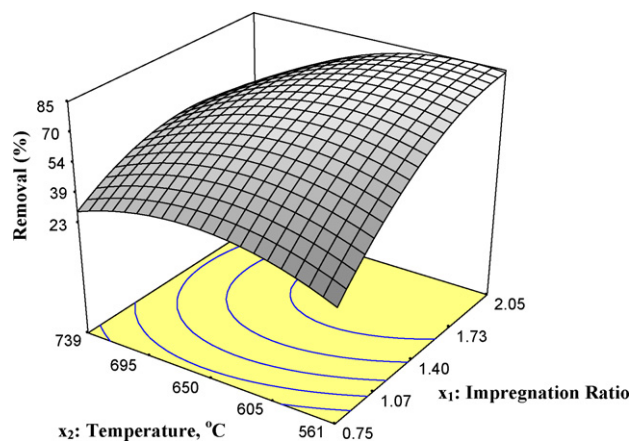


Fig. 1. A three-dimensional response surface plot for effect of temperature and impregnation on MB removal by WTAC at fixed time $t = 105$ min.

x_2x_3 were insignificant. A good correlation existed between the predicted and experimental data (fig. not shown) with a correlation coefficient R^2 of 0.94.

The F -value and $\text{Prob} > F$ for the MB and AB29 removal response as adjudged by the ANOVA analysis were 11.78, 0.0003 and 13.69, 0.0002, respectively. The MB removal by WTAC model had x_1 , x_2 , x_1^2 and x_2^2 as significant terms while x_2 , x_3 , x_1^2 , x_2^2 and x_2x_3 were significant in AB29 model. Both models had good correlations between the predicted and experimental data for their removal by WTAC. The correlation coefficients R^2 supporting the co-ordination between the optimization variables and the responses in respect to the predicted and experimental data were graphically represented and the values were 0.91 for MB and 0.92 for AB29 (figs. not shown).

The three variables IR, temperature of activation and activation time all contributed either individually or by way of interaction to the removal of both MB and AB29 by WTAC, although their level of contributions differed. The IR and activation temperature imposed the most significant effect on the removal of MB by WTAC. This was shown by their largest F -values by either one factor approach (x_1 , x_2) or by interaction between the factors x_1x_2 as shown in Table 3. Their interaction effect on MB removal by WTAC is shown on the three-dimensional surface response analysis presented in Fig. 1. This represents impregnation ratio and temperature interaction when time was fixed at zero level ($t = 105$ min). Activation time showed the least effect on the removal of AB29 dye by the WTAC. The observed high removal of both MB and AB29 by WTAC was proportional to increase in IR and activation temperature as seen in their quadratic effect in the resulting models. Activation temperature and IR helped in the development of pores and surface area of the adsorbent which contributed to the adsorption of the dyes. Intercalation of potassium metal ion on carbon materials at high temperatures which helps in surface area development, are attributes of potassium compounds activating agents [4]. However, at the highest IR of 2.5, temperature of 650 °C and activation time of 105 min, removal of both MB and AB29 by WTAC was low; this was due to gasification reaction between the excess potassium acetate and the carbon material resulting in the loss of some carbon and also translating to poor development of the pores and its surface area. The non-performance or insignificant activation time variable impact on uptake of MB has been observed by a number of researchers. Gratuito et al. [6] and Sentorun-Shalaby et al. [12] reported that activation time or prolonging time of activation does not necessary lead to yielding of high surface area and enlargement of pores during production of activated carbon.

The removal of AB29 by WTAC as analyzed by ANOVA revealed that temperature distinctively and significantly contributed to its removal more compared with the other variables activation

Table 3
ANOVA for response surface quadratic model for MB removal by WTAC.

Source	Sum of squares	Degree of freedom	Mean square	F-value	Prob > F
Model	12213.49	9	1357.05	11.78	0.0003
x_1	596.69	1	596.69	5.18	0.0461
x_2	7814.89	1	7814.89	67.82	<0.0001
x_3	235.28	1	235.28	2.04	0.1835
x_1^2	629.98	1	629.98	5.74	0.0416
x_2^2	2054.68	1	2054.68	22.82	0.0007
x_3^2	228.17	1	228.17	1.98	0.1897
x_1x_2	124.66	1	124.66	1.08	0.3228
x_1x_3	205.03	1	205.03	1.78	0.2118
x_2x_3	503.71	1	503.71	4.37	0.0630
Residual	1152.33	10	115.23	–	–

Table 4
ANOVA for response surface quadratic model for AB29 removal by WTAC.

Source	Sum of square	Degree of freedom	Mean square	F-value	Prob > F
Model	8976.19	9	997.35	13.69	0.0002
x_1	84.36	1	84.36	1.16	0.3072
x_2	6718.23	1	6718.23	92.19	<0.0001
x_3	545.12	1	545.12	7.48	0.0210
x_1^2	376.71	1	376.71	5.17	0.0463
x_2^2	364.47	1	364.47	5.00	0.0493
x_3^2	49.95	1	49.95	0.69	0.4270
x_1x_2	26.79	1	26.79	0.37	0.5578
x_1x_3	11.66	1	11.66	0.16	0.6975
x_2x_3	716.69	1	716.69	9.84	0.0106
Residual	728.70	10	72.87	–	–

time and impregnation ratio. This was seen in the quantum of their *F*-values of 92.19, 7.48 and 1.16 for temperature, time and IR, respectively; as shown in Table 4. The contribution was attributed to the high temperature needed for pores development and intercalation of potassium metal to the carbon material during activation [5]. Poor adsorption noticed at lower temperature of activation showed that the pores of the waste tea were not properly developed. Quadratic effect of the parameters towards adsorption of AB29 was impacted by the temperature and IR. The three-dimensional graph showing their interaction effect is presented in Fig. 2. Although some parameters were more outstanding in contributing to the removal of AB29 dye by WTAC, other parameters studied also gave their latent contributions.

The analyzed results for the yield of WTAC showed that the three factors had a significant effect on the response with the greatest effect impacted by the interaction of IR and temperature. The least or insignificant effect on the response was as a result of the interaction between the activation time and temperature as shown in Fig. 3(b) with IR fixed at zero level (IR = 1.4). The three-dimensional response surfaces for the activation temperature and IR when time was fixed at zero level ($t = 105$ min) is presented in Fig. 3(a). Activated carbon preparation through chemical activation is achieved by volatilization of the volatile matters in the precursor and loss of some carbon materials through series of reaction mechanisms; this is possible at high temperatures in the presence of ample IR. The presence of the chemical initiates the reactions which are catalyzed through increase in concentration and temperature. Ahmad and Alrozi [9] has reported similar result for study of preparation conditions of activated carbons from mangosteen peel for the removal of Remazol Brilliant Blue R. Activation time had little effect on the yield of the activated carbon produced, this is was in agreement with the effect time had on yield during optimization of activated carbon for the removal of disperse dye [13]. Activation time and temperature interaction produced little effect on the response since only dehydration operation could occur without and any unit process due to the absence of activating agent to ignite the reaction needed. The result for ANOVA analysis on preparation parameter is shown in Table 5.

3.3. Process optimization

Some major variables used for preparation of activated carbons: activation temperature, impregnation ratio and activation time were considered for development of WTAC to optimize the percentage yield and its use for removal of both MB and AB 29. Design Expert software version 6.0.6 (STAT-EASE Inc., Minneapolis, USA) was used to alleviate common problems faced when more than one goal is targeted such as yield and percentage removal with concurrent optimization in place. The relationship of the two

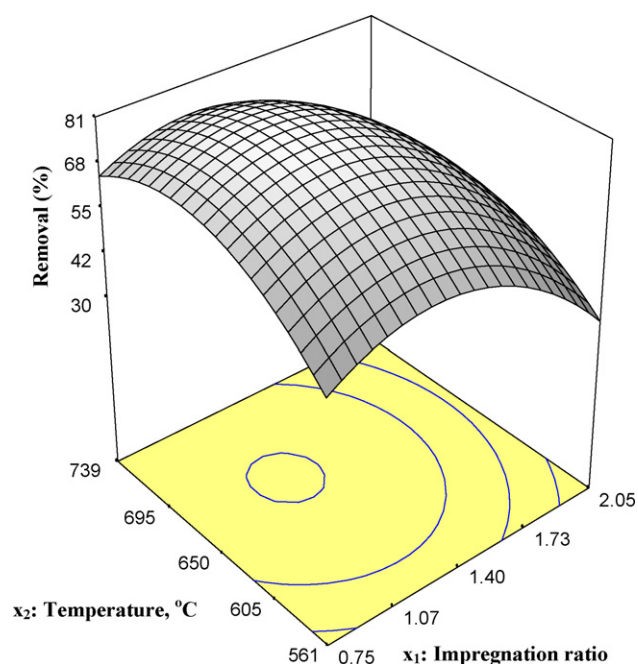


Fig. 2. A three-dimensional response surface plot for effect of temperature and impregnation on AB29 removal by WTAC.

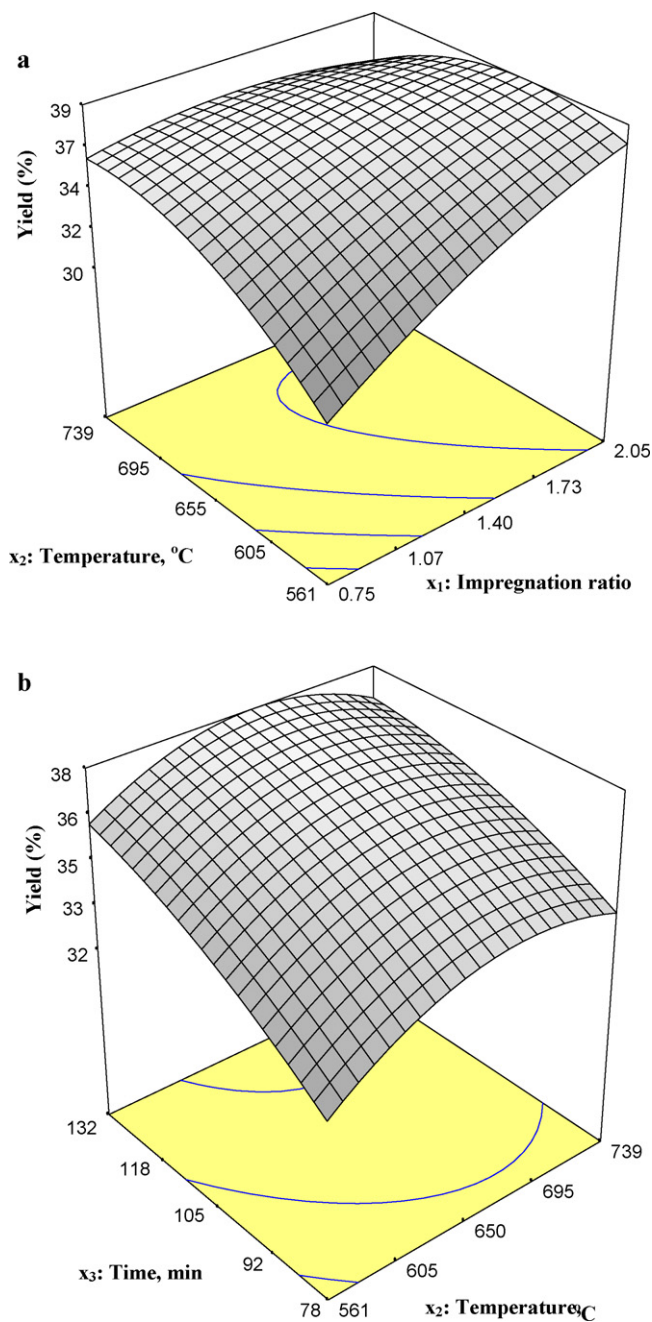


Fig. 3. Three-dimensional response surface plots for yield of WTAC: (a) effect of temperature and impregnation ratio and (b) effect of time and temperature.

Table 5
ANOVA for response surface quadratic model for waste tea activated carbon yield.

Source	Sum of squares	Degree of freedom	Mean square	F-value	Prob > F
Model	333.76	9	37.08	7.68	0.0019
x_1	114.69	1	114.69	23.17	0.0007
x_2	26.35	1	26.35	4.86	0.0520
x_3	10.28	1	10.28	1.53	0.2440
x_1^2	73.48	1	73.48	14.63	0.0033
x_2^2	69.59	1	69.59	13.82	0.0040
x_3^2	46.31	1	46.31	9	0.0133
x_1x_2	27.73	1	27.73	5.15	0.0466
x_1x_3	17.46	1	17.46	3.02	0.1128
x_2x_3	3.2	1	3.2	0.066	0.8020
Residual	19.43	10	1.94	–	–

responses makes it practically impossible to target a particular goal as outcome without conceding for the other goal. The software was used to optimize the two responses under same conditions of the variables studied with minimum error. Confirmatory experiments were carried out on the two predicted responses obtained from the software application to check the alliance and its suitability. The results for the yield and percentage removal of MB and AB29 were 27.94, 83.17 and 79.96%, with error of 2.71, 1.02 and 1.49%, which were obtained from the predicted result of 28.72, 84.03 and 78.77%, respectively. The optimal conditions obtained for the variables studied were 800 °C, IR: 1.4 and 120 min. Details of the result analysis are shown in Table 6. Time wastage and cost alleviation can be avoided for optimization of production of high yield WTAC and its use for good adsorption of MB/AB 29 as revealed by the results obtained.

3.4. Characterization of WTAC

One of the most important features of adsorbents is their surface area and porosity. The BET surface area of WTAC was found to be 854.30 m²/g and this can be compared with some commercial activated carbons having surface areas of 331 m²/g [14] and 769 m²/g [15]. The adsorbent was found to be mesoporous (2–50 nm) in nature with average pore diameter D_p of 2.42 nm. A detail of the BET result analysis is shown in Table 7.

The result for experimental determination of pH_{zpc} from various KNO₃ concentrations used (fig. not shown) was 7.4 ± 0.3

Some anonymous impurities as well as volatile components contained in the precursor were texturized using the SEM analysis as shown in Fig. 4. Upon activation of the precursor at high temperature of 800 with IR of 1.4, good pores were developed on the material. This was due to loss of volatile components, carbon in the form of CO and CO₂, and intercalation of the potassium element into the char formed in the process. This is similar to activation of carbon materials using potassium compounds as activating agents [3,4]. The SEM for the precursor and WTAC are shown in Fig. 4(a) and (b).

3.4.1. The FT-IR study of waste tea activated carbon

The FT-IR for the WTAC prepared at optimized conditions for the adsorption of MB and AB29 is presented in Fig. 5. Aromatic primary groups NH₂ and some O–H functional groups were found around 3425.71 cm⁻¹ band width. The C–H stretch found around 3088.46 cm⁻¹ could be attributed to some saturated and unsaturated vinyl/vinylidene groups. Some derivatives of carboxylic acids which usually have wide bands were found between wavelengths of 2500–1497 cm⁻¹. Specifically, O–H intense band stretches around 2500 cm⁻¹, alkynes stretches of C≡C around 2238.17 cm⁻¹ while, wavenumbers of 1678.74 and 1498.97 cm⁻¹ had stretches of C=C, C=O tertiary amides and C–O inorganic

Table 6
Model validation of WTAC preparation parameters and responses.

MD	x_1 , IR	x_2 (°C)	x_3 (min)	Activated carbon yield			Percentage dye removal (%)					
				Predicted	Experimental	Error	Predicted		Experimental		Error	
							MB	AB29	MB	AB29	MB	AB29
1.00	1.4 ± 0.1	800 ± 2	120 ± 3	28.72	27.94	2.71	84.03	78.77	83.17	79.96	1.02	1.49

Table 7
The BET characterization of the optimized waste tea activated carbon.

S_{BET} (m ² /g)	S_{ext} (m ² /g)	$S_{\text{ext}}/S_{\text{BET}}$ (%)	S_{mic} (m ² /g)	$S_{\text{mic}}/S_{\text{BET}}$ (%)	V_{tot} (cm ³ /g)	V_{mic} (cm ³ /g)	$V_{\text{mic}}/V_{\text{tot}}$ (%)	D_p (nm)
854.30	274.38	32.12	579.87	67.88	0.5162	0.3098	60.02	2.42

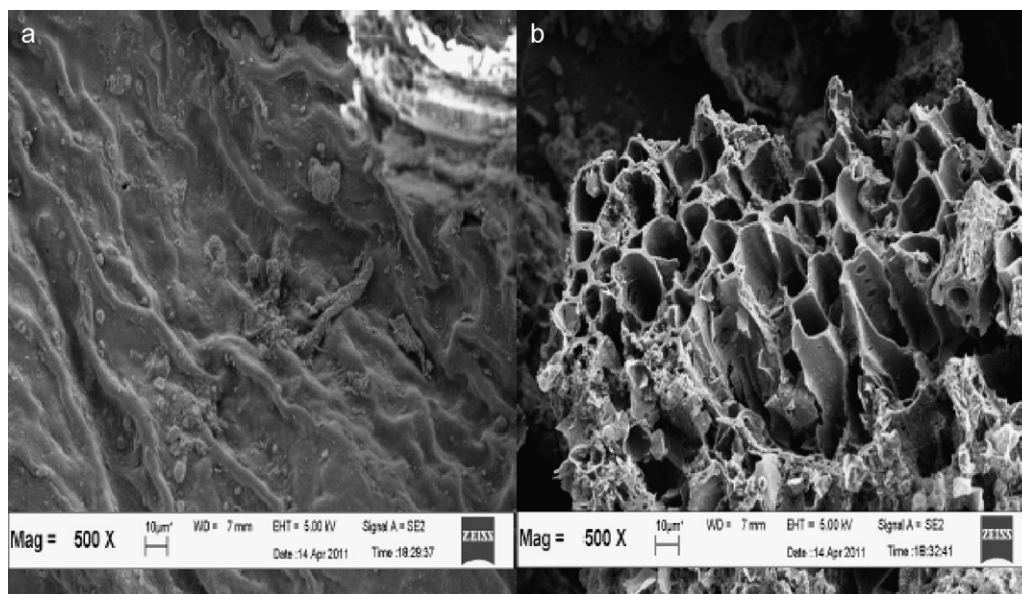


Fig. 4. The SEM of (a) precursor and (b) WTAC of 500× magnification.

carbonates, respectively. El Qada et al. [16] reported that the presence of hydroxyl, alkyl and carbonyl functional groups can dissociate and become negatively charged which will promote electrostatic attraction activities between the negatively charged MB cations and the WTAC surface. Some S–O inorganic sulphates and Si–O–Si asymmetric silica stretches were found at 1132.47 cm⁻¹. Carboxylic acids O–H and meta-benzene bending C–H, were equally found around 955.34 and 759.15 cm⁻¹, respectively. The numerous and varieties of functional groups present in the WTAC adsorbent

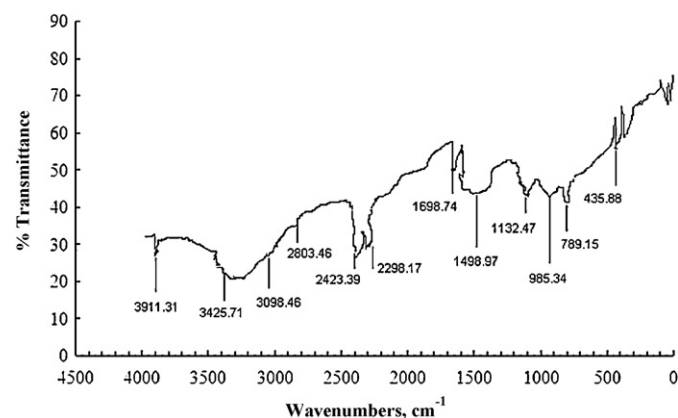


Fig. 5. The FT-IR for waste tea activated carbon.

contributed immensely to its massive adsorption activities for both the MB and AB29 from waste water. The presence of numerous functional groups and their enhancement in adsorption activities in waste tea adsorbents has been reported by other researchers [14,17,18].

3.5. Effect of initial dye concentration

The study of effect of initial dye concentration on the adsorbent adsorption capacity is a useful aspect of adsorption process. This is usually measured when equilibrium position is established between the dye and the adsorbent; that is, the point at which the amount of dye adsorbed on the adsorbent is in a state of dynamic equilibrium with the amount of dye desorbing from the adsorbent.

In this research, initial MB/AB29 concentrations from 50 to 350 mg/L were used to study their adsorption on WTAC. The results revealed that at low concentrations of the dye, equilibrium position was achieved faster while it took longer time for higher initial dye concentrations to attain equilibrium for the two dyes MB and AB29. This could be attributed to the fact that more vacant site were present on the WTAC (adsorbent) with less number of molecules of the adsorbates to occupy and so, the limited available molecules were speedily adsorbed. The results on effect of initial concentration on adsorption of MB and AB29 are presented in Fig. 6(a) and (b). The scenario of longer time for attainment of equilibrium with respect to higher initial dye concentration can be attributed to reasons: firstly, there were more molecules

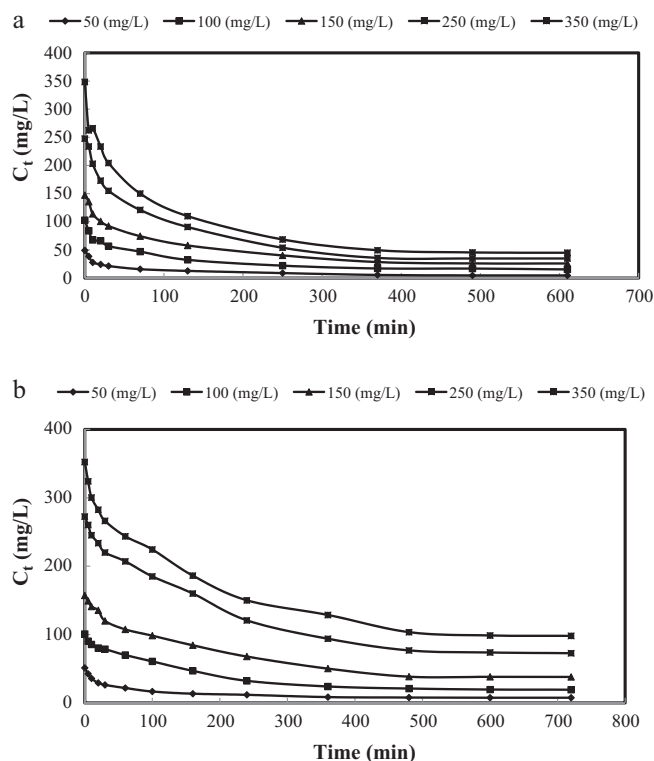


Fig. 6. Effect of initial dye concentration on adsorption at 30 °C: (a) MB and (b) AB29.

of the adsorbates at fixed adsorbent dosage with limited vacant sites which lead to formation of queue of molecules waiting to be adsorbed before saturation. Secondly, the adsorbates had to undergo sequence of some adsorption processes which includes: movement of molecules to the adsorbent external surface through a boundary layer, diffusion of the molecules into the pores of the adsorbent and finally, diffusion of adsorbates onto interior pores of the adsorbent [19,20]. At the initial concentrations of 50–250 mg/L (50 °C) for MB, equilibrium condition was attained after 70 min while at 350 mg/L dye concentration it took 130 min before equilibrium was established. The attainment of equilibrium of AB29 was at 100 min and 240 min for initial concentrations of 50–150 mg/L and 250–350 mg/L, respectively; at 50 °C. Longer time was taken for equilibrium to be established at lower temperature of adsorption for the two dyes at all the initial concentrations; however, equilibrium concentrations were measured at 1440 min. It was also observed that the adsorption capacity at equilibrium for MB and AB29 increases from 43.69 to 310.99 mg/g and 43.28 to 248.29 mg/g, respectively, with initial dye concentration from 50 to 350 mg/L. Therefore, it can be said that adsorption of MB/AB29 on WTAC increased with increase in initial dye concentration. Similar trend was observed in the adsorption of Reactive Blue 15 dye from aqueous solution on cross-linked chitosan beads [21] and also in the adsorption of Methylene Blue on oil palm shell activated carbon [22].

3.6. Effect of pH on adsorption MB and AB29 on WTAC

The effect pH was investigated on the adsorption of MB and AB29 on WTAC at a pH of 2–12 for 12 h. The result in Fig. 7 showed that maximum adsorption of AB29 was obtained at the lowest pH 2 while the lowest adsorption was at pH 12; the reverse was the case for the adsorption of MB. The high adsorption of AB29 can be attributed to electrostatic attraction between the negative charges of the adsorbent surface and the protonated hydrogen ions in the

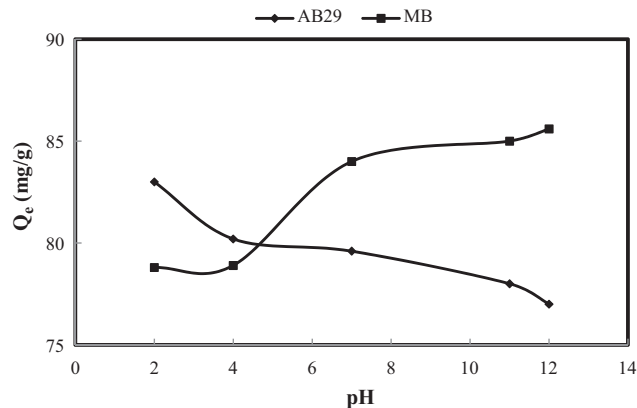


Fig. 7. Effect of pH on adsorption of MB/AB29 on WTAC at 30 °C.

acidic dye solution, while the presence of more negative charges at higher pH promoted the adsorption of MB. As the pH of the solution increases, adsorption of AB29 was found to be decreasing; this was due to extinction of the positive hydrogen ions thereby promoting activities of electrostatic repulsion between the negative charges of both the anionic dye and the WTAC surface [23]. Reduction in adsorption of MB was observed at low pH which was equally attributed to repulsion of positive ions which were more in the acidic medium [24]. The results of the pH effect on the adsorption of the two adsorbates had involvement of ion exchange and electrostatic interaction between the adsorbent and the adsorbates; similar occurrence was observed in pH study of binding of arsenic on dolomite surface [25].

3.7. Adsorption isotherm

Adsorption isotherm studies give information about the distribution of adsorbate between the liquid phase and the solid phase when adsorption process reaches equilibrium. This information helps an Engineer to optimize the design parameters for adsorption system and also helps to establish the most appropriate correlation for equilibrium curves. The equilibrium characteristics of this adsorption study were described through Langmuir, Freundlich and Temkin equations.

The non-linear form of the Langmuir isotherm model [26] is given as:

$$Q_e = \frac{Q_m C_e b}{1 + b C_e} \quad (10)$$

where C_e (mg/L) is the equilibrium concentration of MB/AB29 adsorbed, Q_e (mg/g) is the amount of MB/AB29 adsorbed, Q_m and b (Langmuir constants), the monolayer adsorption capacity and affinity of adsorbent towards adsorbate respectively.

A plot of Q_e against C_e gave a fitted curve (fig. not shown), and the Langmuir constants were generated from the plot of sorption data; the parameters evaluated for the two dyes are shown in Table 8.

The non-linear form of the Freundlich model was used to investigate the adsorption process adherence to the model, the equation [27] is given as:

$$Q_e = k_f C_e^{1/n} \quad (11)$$

where Q_e (mg/g) is the amount of dye adsorbed at equilibrium, C_e (mg/L) is the equilibrium concentration of the adsorbate, k_f and n are the Freundlich equilibrium coefficients. The value of n gives information on favourability of adsorption process and k_f is the adsorption capacity of the adsorbate.

A plot of Q_e against C_e gave poor fitted curves (fig. not shown) indicating that the adsorption process did not follow the model.

Table 8
Langmuir, Freundlich and Temkin isotherm models for MB and AB29 adsorption on WTAC at 30 °C.

Isotherms	Parameters	Methylene Blue			Acid Blue 29		
		30 °C	40 °C	50 °C	30 °C	40 °C	50 °C
Langmuir	Q_m (mg/g)	446.53	472.00	554.30	336.68	437.70	453.12
	b (L/mg)	0.045	0.069	0.031	0.021	0.015	0.026
	R^2	0.818	0.932	0.992	0.963	0.982	0.986
Freundlich	k_f	29.31	37.15	49.81	16.88	17.71	23.69
	$1/n$	0.638	0.527	0.546	0.601	0.558	0.601
	R^2	0.786	0.866	0.986	0.958	0.948	0.949
Temkin	A_T	73.03	94.38	121.69	70.55	89.18	93.99
	b_T (kJ/mol)	0.316	0.820	0.857	0.238	0.171	0.289
	R^2	0.637	0.664	0.944	0.943	0.943	0.941

Equilibrium coefficients k_f and n , values were generated from the plot of sorption data. The parameter $1/n$ gives information on adsorption intensity or surface heterogeneity with values between 0 and 1 becoming more heterogeneous as the value gets closer to zero. The results obtained showed that the adsorption surface of WTAC was heterogeneous in nature from $1/n$ values calculated for the two adsorbates adsorption which were between 0.527 and 0.638; similar results of heterogeneous adsorbents has been reported [28]. The parameters obtained for MB and AB29 adsorption on WTAC are shown in Table 8.

3.7.1. Temkin isotherm

The effect of the two adsorbates interaction with WTAC during adsorption was studied using Temkin isotherm model. The model which was proposed by Temkin and Pyzhev is based on two premises: the increase of coverage due to adsorbate–adsorbent interactions leads to decrease in heat of adsorption of all molecules in the layer; and that adsorption is characterized by a uniform distribution of binding energies up to some maximum binding energy [29]. The Temkin model equation can be expressed as:

$$Q_e = B \ln(K_T C_e) \quad (12)$$

where K_T is the equilibrium binding constant corresponding to the maximum binding energy, B is related to the heat of adsorption, Q_e (mg/g) is the experimental adsorption capacity, C_e (mg/L) is the concentration of the MB/AB29 dye adsorbed at equilibrium position;

$$B = \frac{RT}{b_T} \quad (13)$$

where $1/b_T$ indicates the adsorption potential of the adsorbent; R is the universal gas constant (8.314 J/kmol); and T is the temperature in Kelvin (K).

A plot of Q_e against C_e at various temperatures of operation gave good curves for both MB and AB29 (fig. not shown).

The correlation coefficient R^2 -values as shown in Table 8 (MB and AB29) revealed that Langmuir isotherm model best described the adsorption of both MB and AB29 on WTAC. The maximum adsorption capacity for MB and AB29 removal by WTAC were 554.30 and 453.12 mg/g, respectively. The higher adsorption of MB by the WTAC can be attributed to two reasons: (1) more the adsorbent was slightly more negatively charged as revealed by the pHzpc studies thereby promoting binding of cationic MB to the surface of WTAC; and (2) the smaller molecular weight of MB (319.85 g/mol) as compared with that of AB29 (616.49 g/mol), enhanced its rate of adsorption and larger adsorption per gram of the adsorbent which was in agreement with Graham's law of diffusion [30]. This is comparable with other adsorbents reported in literature as can be seen in Table 9.

3.8. Adsorption kinetic studies

3.8.1. Pseudo-first order model

The non-linear form of pseudo-first order equation [35] is given as:

$$Q_t = Q_e(1 - e^{-K_1 t}) \quad (14)$$

where Q_e and Q_t are the amount of MB/AB29 dye adsorbed (mg/g) at equilibrium and at time t (h), respectively; K_1 is the rate constant of adsorption (h^{-1}). Plots of Q_t against Q_e , at various temperatures studied were plotted (figs. not shown) for the two adsorbates and the parameters obtained are presented in Table 10.

3.8.2. Pseudo-second order model

The pseudo-second order equilibrium adsorption model [36] can be calculated using the equation:

$$Q_t = \frac{K_2 Q_e^2 t}{(1 + K_2 Q_e t)} \quad (15)$$

where K_2 (g/(mg h)) is the rate constant of second order adsorption. Plots of Q_t versus t at various temperatures studied gave very good curves as shown in Fig. 8(a) and (b). The pseudo-second-order parameters generated from the plots for adsorption of MB and AB29 on WTAC are tabulated in Table 10.

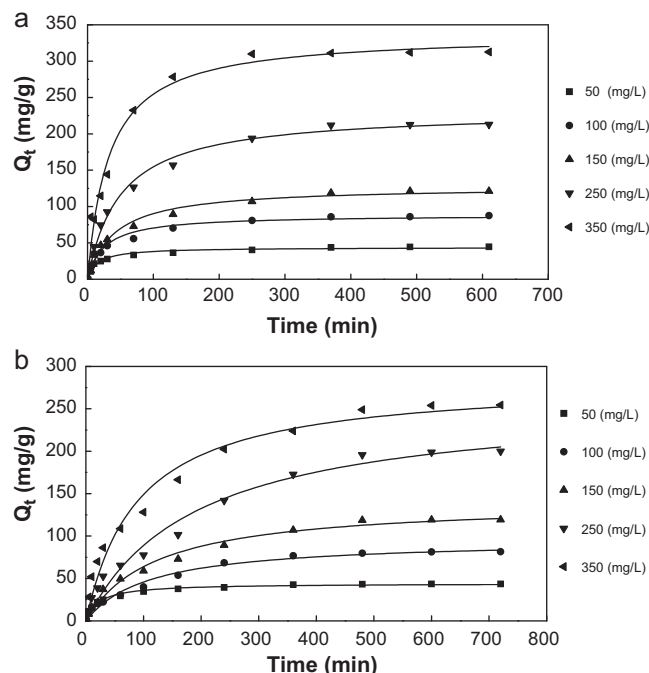


Fig. 8. Pseudo-second-order kinetics plot at 30 °C for (a) MB and (b) AB29.

Table 9
Adsorption capacity of different adsorbents for anionic and acidic dye adsorption.

Adsorbents	Dyes	Maximum monolayer adsorption capacities (mg/g)	Reference
WTAC	Methylene Blue	554.30	This work
WTAC	Acid Blue 29	453.12	This work
DTMA–Bentonite	Acid Blue 193	740.5	[14]
PEI-modified <i>Penicillium chrysogenum</i> biomass	Acid Orange 8	352	[15]
PEI-modified <i>Penicillium chrysogenum</i> biomass	Acid Blue 45	196	[15]
Papaya seed	Methylene Blue	555.56	[24]
Mesoporous granular pine-cone derived activated carbon	Acid Black 1	452.98	[31]
Mesoporous granular pine-cone derived activated carbon	Acid Blue 113	298.4	[31]
Tea waste	Methylene Blue	85.16	[32]
Diatomite	Methylene Blue	156.6	[33]
RPAC	Malachite Green	329.49	[34]

Table 10
Pseudo-first-order and second-order kinetic analysis for MB and AB29 adsorption on WTAC at 30 °C.

Dye	Dye conc. (mg/L)	Q_{exp} (mg/g)	Pseudo-first-order			Pseudo-second-order		
			Parameters		R^2	Parameters		R^2
			K_1 (h ⁻¹)	Q_{cal}		K_2 ($\times 10^5$)	Q_{cal}	
MB	50	43.280	0.3200	40.73	0.970	99.20	44.22	0.999
	100	79.794	0.0079	81.05	0.979	9.46	96.18	0.988
	150	118.831	0.0073	117.91	0.978	5.87	141.04	0.991
	250	195.793	0.0052	205.65	0.976	2.00	259.72	0.970
	350	248.992	0.0088	245.05	0.994	3.89	283.85	0.990
AB29	50	43.685	0.0488	40.74	0.928	45.20	43.87	0.998
	100	85.794	0.0282	81.27	0.990	43.90	88.57	0.998
	150	119.944	0.0186	114.34	0.979	18.80	127.72	0.997
	250	211.793	0.0159	205.24	0.986	8.62	231.87	0.996
	350	310.992	0.0230	307.16	0.981	0.91	337.32	0.998

The two kinetic models studied fitted well with the adsorption of the anionic and cationic dyes going by the correlation coefficients R^2 which were all above 0.900. Even though high R^2 -values for the two kinetic models on adsorption of the two dyes emanated, and the fact that results of correlation coefficient is not a sufficient criteria for selection of an adsorption kinetic model [37]; the pseudo-second-order kinetic model described best the adsorption process. The second-order kinetic model had the least R^2 of 0.97 while the highest value of R^2 for pseudo-first-order kinetic was 0.994 for the two adsorbates. Generally, pseudo-second-order kinetic correlation coefficient R^2 -values were all more tending towards unity.

3.9. Adsorption thermodynamics

Thermodynamic parameters for adsorption of MB/AB29 on WTAC were undertaken at various temperatures of 30, 40 and 50 °C. This was done to determine the spontaneity of the adsorption process. The equation used is expressed as:

$$\Delta G = -RT \ln K_0 \quad (16)$$

where R is the universal gas constant (8.314 J/kmol); T is the absolute temperature (K); K_0 is the distribution coefficient expressed as $K_0 = Q_e/C_e$; and ΔG is the Gibbs free energy.

Van't Hoff equation was used to determine the average standard enthalpy change, the equation is expressed as:

$$\ln K_0 = \frac{-\Delta G}{RT} = \frac{\Delta S}{R} - \frac{\Delta H}{RT} \quad (17)$$

A plot of $\ln K_0$ against $1/T$ gives a graph (fig. not shown) where we can obtain ΔS from the intercept and ΔH from the slope.

Thermodynamic parameters results for the adsorption of the two dyes MB and AB29 on WTAC at various temperatures under study are reported in Table 11. The adsorption processes were both spontaneous in nature as the analysis all resulted in negative values

Table 11
Thermodynamic parameters of MB and AB29 adsorption on WTAC at 150 mg/L.

Dye	ΔH (kJ/mol)	ΔS (J/mol)	ΔG (kJ/mol)		
			303 K	313 K	323 K
MB	10.871	45.7	-7.796	-10.663	-10.797
AB29	27.120	109.99	-6.391	-6.870	-8.565

of change of Gibbs free energy (ΔG). The positive values of both enthalpy (ΔH) and entropy (ΔS) obtained for both MB and AD29 adsorption on WTAC showed that the adsorption processes were endothermic and all had random characteristics. This has further confirmed the results of the studies on effect of temperature on the adsorption in Section 3.8. The absolute value of change of Gibbs free energy for physical adsorption is -20 to 0 kJ/mol which is smaller than that of chemisorptions -80 to -400 kJ/mol [38,39]. Results of Gibbs free energy of this study further affirmed that the adsorption processes were physical in nature. Similar results were reported for adsorption of Basic Black dye using calcium alginate beads [40].

4. Conclusions

A central composite design was used to optimize the production of high yield of WTAC and its use for removal of MB and AB29 at various parameters such as activation temperature, impregnation ratio and activation time under study. The optimal parameters conditions obtained were 800 °C, IR 1.4 and 120 min which translated to 27.94, 83.17 and 79.96% for the yield, MB and AB29 removal, respectively. Activation temperature and chemical impregnation ratio from the three parameters studied were found to have the greatest impact on both the yield of WTAC and its use for uptake of MB/AB 29. Freundlich isotherm model described best the adsorption process and pseudo-second-order kinetic model was more fitting to the adsorption data obtained for both MB/AB29 adsorptions on WTAC. Textural characterization of the WTAC showed that the BET

surface area was 854.25 m²/g, total pore volume of 0.52 cm³/g and an average pore diameter of 2.42 nm. The optimization analysis has revealed that high yield of activated carbon for good removal of MB and AB29 can be prepared from waste tea which is comparable to some conventional commercial activated carbon.

Acknowledgements

The authors acknowledge the financial support provided by Universiti Sains Malaysia under the Research University (RU) Scheme (Project No. 1001/PJKIMIA/814072).

References

- [1] Y. Al-Degs, M.A.M. Khraisheh, S.J. Allen, M.N. Ahmad, G.M. Walker, Competitive adsorption of reactive dyes from solution: equilibrium isotherm studies in single and multisolute systems, *Chem. Eng. J.* 128 (2007) 163–167.
- [2] N.K. Amin, Removal of Direct Blue-106 dye from aqueous solution using new activated carbons developed from pomegranate peel: adsorption equilibrium and kinetics, *J. Hazard. Mater.* 165 (2009) 52–62.
- [3] J. Hayashi, T. Horikawa, I. Takeda, K. Muroyama, F.N. Ani, Preparing activated carbon from various nutshells by chemical activation with K₂CO₃, *Carbon* 40 (2002) 2381–2386.
- [4] M. Auta, B.H. Hameed, Preparation of waste tea activated carbon using potassium acetate as an activating agent for adsorption of Acid Blue 25 dye, *Chem. Eng. J.* 171 (2011) 502–509.
- [5] H. Dolas, O. Sahin, C. Saka, H. Demir, A new method on producing high surface area activated carbon: the effect of salt on the surface area and the pore size distribution of activated carbon prepared from pistachio shell, *Chem. Eng. J.* 166 (2011) 191–197.
- [6] M.K.B. Gratuito, T. Panyathanmaporn, R.-A. Chumnanklang, N. Sirinuntawitaya, A. Dutta, Production of activated carbon from coconut shell: optimization using response surface methodology, *Bioresour. Technol.* 99 (2008) 4887–4895.
- [7] B.H. Hameed, I.A.W. Tan, A.L. Ahmad, Optimization of basic dye removal by oil palm fibre-based activated carbon using response surface methodology, *J. Hazard. Mater.* 158 (2008) 324–332.
- [8] I.A.W. Tan, A.L. Ahmad, B.H. Hameed, Preparation of activated carbon from coconut husk: optimization study on removal of 2,4,6-trichlorophenol using response surface methodology, *J. Hazard. Mater.* 153 (2008) 709–717.
- [9] M.A. Ahmad, R. Alrozi, Optimization of preparation conditions for mangosteen peel-based activated carbons for the removal of Remazol Brilliant Blue R using response surface methodology, *Chem. Eng. J.* 165 (2010) 883–890.
- [10] N. Dafale, S. Wate, S. Meshram, T. Nandy, Kinetic study approach of Remazol Black-B use for the development of two-stage anoxic–oxic reactor for decolorization/biodegradation of azo dyes by activated bacterial consortium, *J. Hazard. Mater.* 159 (2008) 319–328.
- [11] Y.S. Al-Degs, M.I. El-Barghouthi, A.H. El-Sheikh, G.M. Walker, Effect of solution pH, ionic strength, and temperature on adsorption behavior of reactive dyes on activated carbon, *Dyes Pigment* 77 (2008) 16–23.
- [12] C. Sentorun-Shalaby, M.G. Ucak-Astarlioglu, L. Artok, C. Sarici, Preparation and characterization of activated carbons by one-step steam pyrolysis/activation from apricot stones, *Micropor. Mesopor. Mater.* 88 (2006) 126–134.
- [13] A.A. Ahmad, B.H. Hameed, A.L. Ahmad, Removal of disperse dye from aqueous solution using waste-derived activated carbon: optimization study, *J. Hazard. Mater.* 170 (2009) 612–619.
- [14] A.S. Özcan, E. Bilge, O. Adnan, Adsorption of Acid Blue 193 from aqueous solutions onto Na-bentonite and DTMA-bentonite, *J. Colloid Interface Sci.* 280 (2004) 44–54.
- [15] B. Low, Y. Ting, S. Deng, Surface modification of *Penicillium chrysogenum* mycelium for enhanced anionic dye removal, *Chem. Eng. J.* 141 (2008) 9–17.
- [16] E.N. El Qada, S.J. Allen, G.M. Walker, Adsorption of basic dyes from aqueous solution onto activated carbons, *Chem. Eng. J.* 135 (2008) 174–184.
- [17] C. Duran, D. Ozdes, A. Gundogdu, M. Imamoglu, H.B. Senturka, Tea-industry waste activated carbon, as a novel adsorbent, for separation, preconcentration and speciation of chromium, *Anal. Chim. Acta* 688 (2011) 75–83.
- [18] M. Ahmaruzzaman, S. Laxmi Gayatri, Activated tea waste as a potential low-cost adsorbent for the removal of *p*-nitrophenol from wastewater, *J. Chem. Eng. Data* 55 (2010) 4614–4623.
- [19] A. Mittal, V. Gajbe, J. Mittal, Removal and recovery of hazardous triphenylmethane dye, Methyl Violet through adsorption over granulated waste materials, *J. Hazard. Mater.* 150 (2008) 364–375.
- [20] L.G.T. dos Reis, N.F. Robaina, W.F. Pacheco, R.J. Cassella, Separation of Malachite Green and Methyl Green cationic dyes from aqueous medium by adsorption on Amberlite XAD-2 and XAD-4 resins using sodium dodecylsulfate as carrier, *Chem. Eng. J.* 171 (2011) 532–540.
- [21] M.S. Chiou, G.S. Chuang, Competitive adsorption of dye metanil yellow and RB 15 in acid solutions on chemically cross-linked chitosan beads, *Chemosphere* 62 (2006) 731–740.
- [22] I.A.W. Tan, A.L. Ahmad, B.H. Hameed, Adsorption of basic dye using activated carbon prepared from oil palm shell: batch and fixed bed studies, *Desalination* 225 (2008) 13–28.
- [23] K. Badii, F.D. Ardjani, M.A. Saberi, N.Y. Limaee, S.Z. Shifaei, Adsorption of Acid Blue 25 on diatomite in aqueous solutions, *Indian J. Chem. Technol.* 17 (2010) 7–16.
- [24] B.H. Hameed, Evaluation of papaya seeds as a novel non-conventional low-cost adsorbent for removal of Methylene Blue, *J. Hazard. Mater.* 162 (2009) 939–944.
- [25] Y. Salameh, N. Al-Lagtah, M.N.M. Ahmad, S.J. Allen, G.M. Walker, Kinetic and thermodynamic investigations on arsenic adsorption onto dolomitic sorbents, *Chem. Eng. J.* 160 (2010) 440–446.
- [26] I. Langmuir, The constitution and fundamental properties of solids and liquids, *J. Am. Chem. Soc.* 38 (1916) 2221–2295.
- [27] H.M.F. Freundlich, Over the adsorption in solution, *J. Phys. Chem.* 57 (1906) 385–470.
- [28] A. Duffy, G.M. Walker, S.J. Allen, Investigations on the adsorption of acidic gases using activated dolomite, *Chem. Eng. J.* 117 (2006) 239–244.
- [29] M.J. Temkin, V. Pyzhev, Recent modifications to Langmuir isotherms, *Acta Physicochem. USSR* 12 (1940) 217–225.
- [30] W.W. Eckenfelder, *Industrial Water Pollution Control*, 3rd ed., McGraw-Hill Companies Inc., USA, 2000.
- [31] M. Hadi, M.R. Samarghandi, G. McKay, Equilibrium two-parameter isotherms of acid dyes sorption by activated carbons: study of residual errors, *Chem. Eng. J.* 160 (2010) 408–416.
- [32] M.T. Uddin, M.A. Islam, S. Mahmud, M. Rukanuzzaman, Adsorptive removal of Methylene Blue by tea waste, *J. Hazard. Mater.* 164 (2009) 53–60.
- [33] M.A. Al-Ghouti, M.A.M. Khraisheh, S.J. Allen, M.N. Ahmad, The removal of dyes from textile wastewater: a study of the physical characteristics and adsorption mechanisms of diatomaceous earth, *J. Environ. Manage.* 69 (2003) 229–238.
- [34] M.A. Ahmad, R. Alrozi, Removal of malachite green dye from aqueous solution using rambutan peel-based activated carbon: equilibrium, kinetic and thermodynamic studies, *Chem. Eng. J.* 171 (2011) 510–516.
- [35] S. Lagergren, B.K. Svenska, On the theory of so-called adsorption of dissolved substances, *The Royal Swedish Academy of Sciences Document*, Band 24 (1898) 1–13.
- [36] Y.S. Ho, S. McKay, Pseudo-second order model for sorption processes, *Process Biochem.* 34 (1999) 451–465.
- [37] S. Azizian, B. Yahyaee, Adsorption of 18-crown-6 from aqueous solution on granular activated carbon: a kinetic modeling study, *J. Colloid Interface Sci.* 299 (2006) 112–115.
- [38] M.J. Jaycock, G.D. Parfitt, *Chemistry of Interfaces*, Ellis Horwood, Onichester, 1981, pp. 12–13.
- [39] Q. Li, Q. Yue, Y. Su, B. Gao, H. Sun, Equilibrium, thermodynamics and process design to minimize adsorbent amount for the adsorption of acid dyes onto cationic polymer-loaded bentonite, *Chem. Eng. J.* 158 (2010) 489–497.
- [40] R. Aravindhan, N.N. Fathima, J.R. Rao, B.U. Nair, Equilibrium and thermodynamic studies on the removal of Basic Black dye using calcium alginate beads, *Colloid Surf. A: Physicochem. Eng. Aspects* 299 (2007) 232–238.